Ab Initio Calculations of the Reactions of Hydrogen with Methanol: A Comparison of the Role of Bond Distortions and Pauli Repulsions on the Intrinsic Barriers for Chemical Reactions

Paul Blowers, Laura Ford, and Rich Masel*

Department of Chemical Engineering, University of Illinois at Urbana-Champaign, Urbana, Illinois 61801-3792

Received: April 29, 1998; In Final Form: July 8, 1998

People often view barriers to reaction as being associated with either bond stretching and distortion or with curve-crossings on a potential energy surface. However, another important contribution to barriers to reaction comes from the energy required to push the reactants together. In this paper we used ab initio methods at various levels including G2.MP2/6-31G* and QCISD(T)/6-311g** to assess the contributions from bond distortions, the curve-crossing, and the energies to move the reactants together for the following reactions: $H' + CH_3OH \rightarrow HH' + CH_2OH$; $H' + CH_3OH \rightarrow HH' + CH_3O$; $H' + CH_3OH \rightarrow H + CH_2H'OH$; $H' + CH_3OH \rightarrow H + CH_3OH'$; $H' + CH_3OH \rightarrow CH_3H' + OH$; $H' + CH_3OH \rightarrow CH_3 + OHH$. We find that the activation barriers correlate very well with the energy to move the reactants together. However, there is little correlation between the activation barriers and either the energy of the curve-crossing or the bond distortion energy. Physically, orbitals distort when the reactants come together. These distorted orbitals have contributions from many states which are not occupied in either the reactants or products. As a result, the physical picture of the reaction as a curve-crossing does not work. We provide a new physical picture in this paper, where the main barrier to reaction is associated with bringing the reactants together and populating the states which are not occupied in either the reactants or products. In this picture, bond distortion lowers the barriers to reaction by reducing the stresses associated with orbital overlap between the reactants. At this point, we do not know if these are general results or results specific to these reactions. However, if they are general, then the ideas we use to think about a reaction, or a reaction coordinate, will need to be rethought.

Introduction

In the literature, people often say that reactions are activated because it costs energy to stretch and break bonds.[1−4] Years ago, Johnston[1] showed that he could correlate the barriers to reaction to the energy of bond stretching calculated via a BEBO relationship. Evans and Polanyi[2] used similar ideas to derive the Evans−Polanyi relationship. Szabo[3] used the same concept to model a variety of reactions. Later investigators used the degree of bond distortion as a reaction coordinate,[5] and to support the curve-crossing model. These ideas have also made it into most of the current kinetics and catalysis textbooks, including, unfortunately, mine.[6−9] Quantum calculations have shown that bond stretching and distortions were associated with barriers to chemical reactions. For example, Mitchell et al.[10,11] examined a series of reactions of the form:

$$X + CH_3Y \rightarrow XCH_3 + Y \qquad (1)$$

at the HF/4-31g level and found that there was a correlation between the barrier to reaction and the energy to distort bonds. Essentially, Mitchell found that $E_{distort} - E_A$ was approximately constant, where $E_{distort}$ is the distortion energy and E_A is the activation energy. This leads to the conclusion that bond distortion energies were causing the barriers to reactions.

Over the years there have been a few papers that associated barriers with orbital distortions rather than bond distortions. The work of Goddard et al.[12] is an example. However, these papers have been the exception in the literature.

Recently[13−15] we were examining a series of nonidentity reactions of the form

$$X + CH_3R \rightarrow XCH_3 + R \qquad (2)$$

$$X + CH_3R \rightarrow XH + CH_2R \qquad (3)$$

with X = H and R = CH_3, C_2H_5, CH_2NH_2, CH_2CF_3, and $CH_2C_6H_5$, and we were surprised to find that the orbital distortions were much smaller than in previous calculations. The barriers to reaction 3 were 30 kcal/mol smaller than they were in reaction 2 even though the bond distortion energy was always larger in reaction 3 than in reaction 2. Our results suggested that Pauli repulsions of the type discussed by Goddard and coworkers[12] were controlling the barriers to reaction.

In this paper, we examine the reactions between hydrogen and methanol to see the relative contributions of Pauli repulsions and bond distortions to the reaction barrier. Recall that there are six possible reactions between hydrogen and methanol. These six reactions are

* To whom correspondence should be addressed.

10.1021/jp982056+ CCC: $15.00
Published on Web 10/28/1998

$$H' + CH_3OH \rightarrow HH' + CH_2OH \quad (4)$$

$$H' + CH_3OH \rightarrow HH' + CH_3O \quad (5)$$

$$H' + CH_3OH \rightarrow H + CH_2H'OH \quad (6)$$

$$H' + CH_3OH \rightarrow H + CH_3OH' \quad (7)$$

$$H' + CH_3OH \rightarrow CH_3H' + OH \quad (8)$$

$$H' + CH_3OH \rightarrow CH_3 + OHH' \quad (9)$$

In the gas phase one normally sees reaction 4.[16,17] However, analogs of reactions 4 and 5 are normally seen on surfaces.[18,19] Reaction 9 occurs on acidic surfaces.[20,21] In this paper, we have examined all six reactions by calculating their intrinsic barriers to reactions in the gas phase. We also calculated the deformation energies and the Pauli repulsions to see how much these two terms affect the barriers to reaction.

The calculations were done at the HF, MP2, MP4SDTQ, QCISD(T), B3LYP, and G2 levels of theory. The accuracy of the different levels of calculation are compared through heats of reaction and reaction pathway information.

We find that the Pauli repulsions in bringing the reactions together are larger than everything else and control the barriers to reaction.

Computational Methods

The computations in this paper were done using the Gaussian 92 and Gaussian 94 packages.[22,23] Calculations were done ranging from the HF/6-31g* level up through QCISD(T)/6-311g** at the MP2/6-31g* optimized geometry to calculate heats of reaction and activation energies for the six reaction pathways. Spin projection was used to eliminate spin contamination. In addition, density functional theory calculations at the B3LYP/6-311+g** level were also done. The G2 method of Pople et al.[24] has been shown in the past to reproduce experimental values with great accuracy and is the standard method used to find species' energies. The G2 calculations are compared with the other methods to evaluate predictive ability and accuracy.

The intrinsic activation barriers were found through the use of the Polanyi equation

$$E_a = E_a^\circ + \gamma \Delta H \quad (10)$$

where E_a is the activation energy, E_a° is the intrinsic activation barrier, γ is the transfer coefficient, and ΔH_{rxn} is the heat of reaction. Intrinsic barriers were also calculated via the Marcus equation.[25]

$$E_a = E_a^\circ\left(1 + \frac{\Delta H_{rxn}}{E_a^\circ}\right)^2 \quad (11)$$

The Bokris method[26] was used to estimate the transfer coefficients.

All transition states were verified to be first-order saddle points through frequency calculations that yielded only one negative eigenvalue. Also, all stable species, including complexes, were verified to have no negative eigenvalues or frequencies. Energies of all transition states, products, and reactants at all levels of calculation are available as supplementary material.

TABLE 1: Activation Energy, Heat of Reaction, and Intrinsic Barriers by Calculational Method (kcal/mol)

method	reaction	E_a	ΔH_{rxn}	$E_a^\circ{}_{Marcus}$	$E_a^\circ{}_{Bokris}$
PUHF/6-31g*	4	16.74	−3.09	18.25	18.79
	5	14.92	−11.26	20.16	23.37
	6	57.15	0.00	57.15	57.15
	7	53.66	0.00	53.66	53.66
	8	39.09	−29.62	52.87	58.31
	9	40.85	−24.70	52.47	53.46
PMP2/6-31g*	4	16.92	1.37	16.23	16.01
	5	22.69	7.68	18.65	16.93
	6	50.66	0.00	50.66	50.66
	7	41.00	0.00	41.00	41.00
	8	41.69	−6.75	45.00	46.07
	9	34.17	−14.57	41.13	41.61
MP4SDTQ(FC)/ 6-311g**	4	11.46	−5.13	13.90	14.86
	5	17.19	2.54	15.89	15.28
	6	45.54	0.00	45.54	45.54
	7	30.88	0.00	30.88	30.88
	8	38.16	−15.69	45.67	48.34
	9	29.38	−24.19	40.57	41.74
MP4SDTQ(FC)/6-	4	11.95	−4.46	14.09	14.90
	5	17.74	3.54	15.92	15.09
	6	44.85	0.00	44.85	44.85
	7	32.15	0.00	32.15	32.15
	8	37.38	−12.92	43.61	45.77
	9	30.31	−21.71	40.44	41.40
QCISD(T)/ 6-311g**	4	10.10	−6.13	12.99	14.16
	5	14.90	0.91	14.44	14.22
	6	43.90	0.00	43.90	43.90
	7	30.25	0.00	30.25	30.25
	8	34.95	−16.65	42.87	45.75
	9	30.84	−24.93	42.39	43.57
PMP2/6-311+g (3df,2p)	4	12.04	−2.57	13.29	13.74
	5	21.48	10.82	15.59	13.34
	6	42.36	0.00	42.36	42.36
	7	28.15	0.00	28.15	28.15
	8	33.68	−7.27	37.22	38.39
	9	26.38	−23.83	37.35	38.55
G2	4	8.99	−13.86	15.13	18.17
	5	14.07	−0.64	14.39	14.55
	6	41.55	0.0	41.55	41.55
	7	24.38	0.0	24.38	24.38
	8	31.54	−12.51	37.54	39.66
	9	24.74	−26.52	36.81	38.29
B3LYP/6-311+g**	4	3.31	−9.30	7.21	9.48
	5	6.43	−2.90	7.81	8.60
	6	35.71	0.0	35.71	35.71
	7	18.35	0.0	18.35	18.35
	8	24.49	−18.46	33.07	36.46
	9	15.88	−29.28	28.65	30.83
experiment	4	8.50	−10.20		
	5	NA	−0.20		
	6	NA	0.00		
	7	NA	0.00		
	8	NA	−12.40		
	9	NA	−26.91		

Results: Potential Energy Surfaces

Figure 1 shows slices of the potential energy surfaces at the MP2/6-31g* level for each reaction. Most of the surfaces were calculated by fixing the bond lengths of the forming and breaking bonds and allowing all of the other geometry parameters to optimize to the lowest energy structure. For reactions 5 and 6 we found we had to constrain some of the other bond lengths when the distances were short or else we would jump to a different reaction sheet. However, in most cases we could stay on the right potential sheet without adding any constraints.

All of the potential energy surfaces look very ordinary for S_N2 reactions. There are complexes on the reactant and product pathways, which are linked by the lowest energy pathway passing through the transition state, TS. Because there is

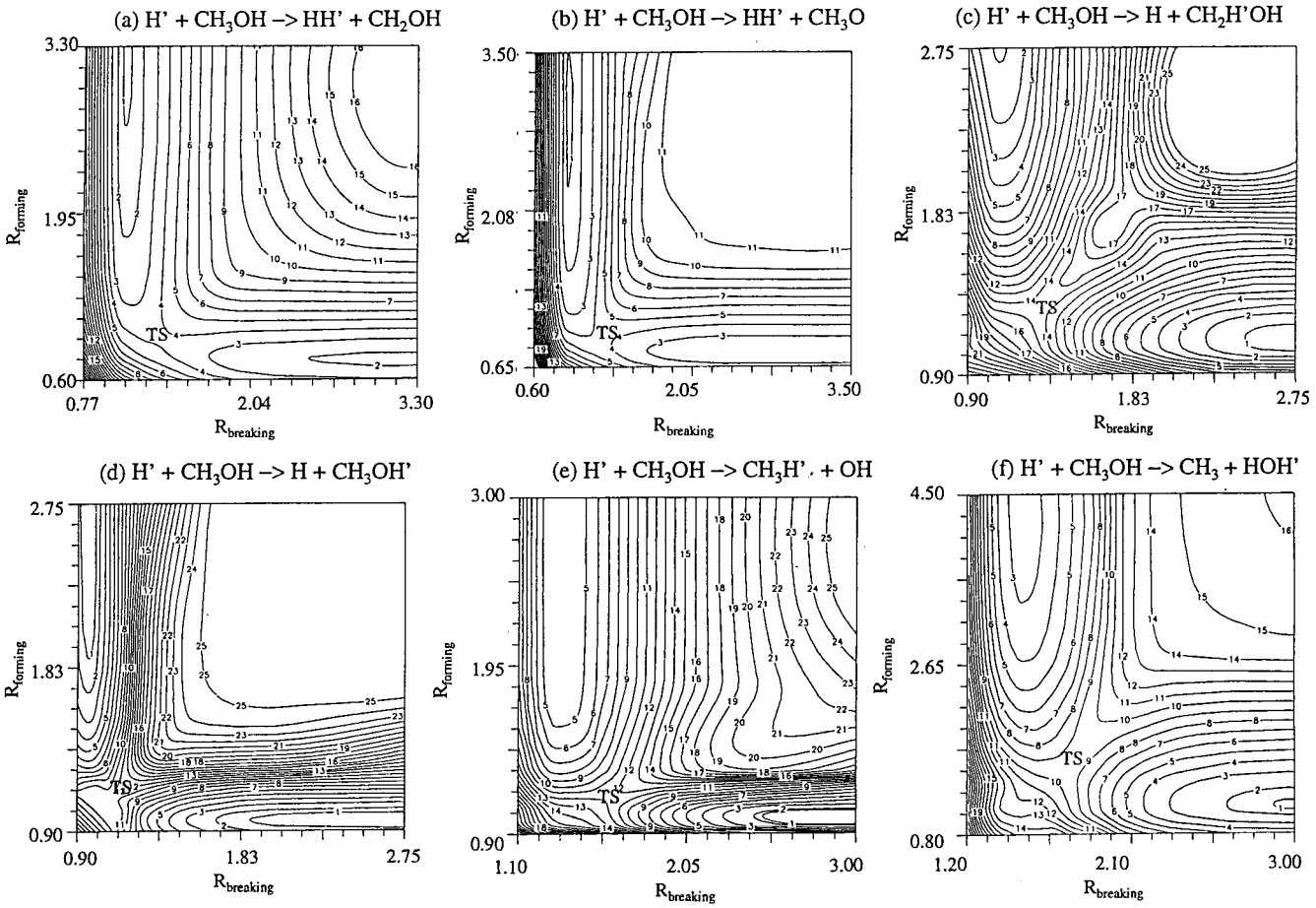

Figure 1. MP2/6-31G* potential energy surfaces for the six reactions (lengths in angstroms) kilocalories/contour: (a) 8, (b) 11, (c) 4, (d) 5, (e) 7, and (f) 5 kcal/mol.

nothing unusual in any of these potential energy surfaces, we thought that these reactions would be good cases to test the bond distortion model.

Results: Barriers

Table 1 shows the activation barriers, heats of reaction, and intrinsic barriers for reactions 4−9 calculated via a variety of methods. The absolute energies of each of the cases is given in the supplemental material. The only reaction with an experimental activation barrier is reaction 4 because it is the only reaction that can be measured in the gas phase. A comparison of the different methods shows that the G2 value of 8.99 kcal/mol comes very close to the experimental value of 8.50 kcal/mol found by Dzotnidze.[16] The density functional theory result is less than half of the experimental value, which was expected based on previous work which has shown that the B3LYP method consistently underpredicts activation barriers.[27] The Hartree−Fock and Moller−Plesset methods, however, overpredict the barrier. This was also expected based on previous work.[28] The MP4 and QCISD(T) methods only slightly overpredict the barrier by a few kcal/mol.

The heat of reaction values allow us to evaluate the accuracy of the calculational methods. Table 2 contains the sum of the absolute errors for each method as compared to the experimental values obtained from the CRC Handbook of Chemistry and Physics.[29] The absolute error is defined as

$$\mathrm{AE} = \sum |\Delta H_{\mathrm{computed}} - \Delta H_{\mathrm{experiment}}| \qquad (12)$$

We see that the PUHF and PMP2 methods both give very large absolute errors of 38 and 37 kcal/mol for these six reactions. The best method for predicting heats of reaction from ab initio calculations is the G2 method, which has an absolute error of only 5 kcal/mol. Surprisingly, the B3LYP method does almost as well as G2.

TABLE 2: Total Absolute Heat of Reaction Error (kcal/mol) by Method

method	total absolute error, (kcal/mol)
PHF/6-31g*	37.60
PMP2/6-31g*	37.44
MP4SDTQ(FC)/6-311g**	13.82
MP4SDTQ(FC)/6-311g(2df,p)	15.20
QCISD(T)/6-311g**	11.41
PMP2/6-311+g(3df,2p)	26.86
G2	4.60
B3LYP/6-311+g**	12.03

The QCISD(T) method also compares quite favorably to the G2 performance. And, as expected, the larger basis set used with the MP4SDTQ(FC) method does slightly better than the smaller PMP2 basis set, with absolute errors of 14 and 15 kcal/mol, respectively.

Table 1 also has a breakdown of results by computational method. This allows a comparison of the ability of each calculational method to predict the same energetic trends. We see that only the Hartree−Fock method incorrectly predicts the lowest barrier pathway. All other methods correctly predict that hydrogen abstraction from carbon will be the preferred pathway, while the HF method predicts hydrogen abstraction from oxygen. The poor performance of this method could be attributed to the very small basis set used, however.

The next highest pathway after hydrogen abstraction from carbon is hydrogen abstraction from oxygen according to the

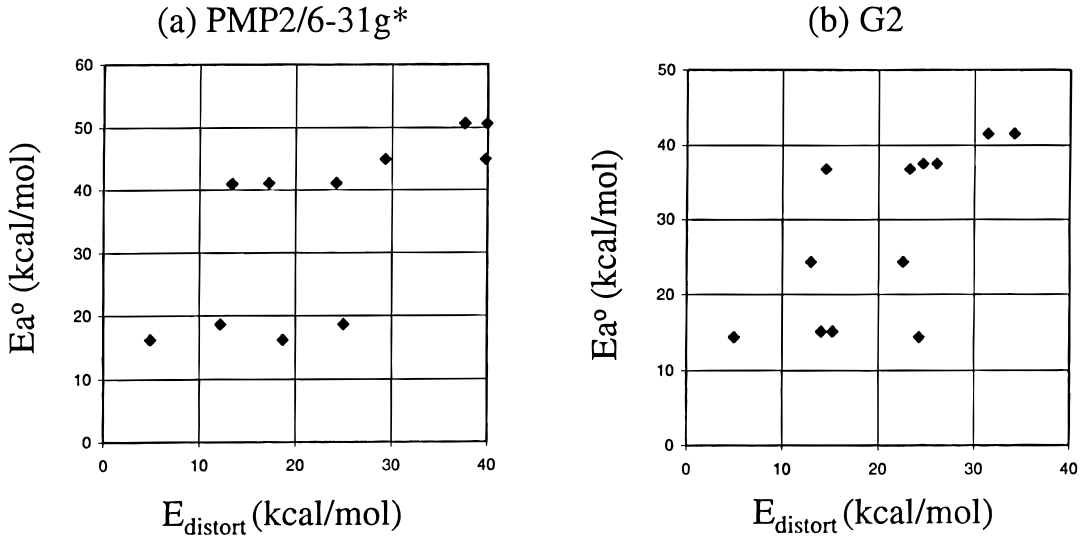

Figure 2. Plot of the intrinsic barriers for reaction as a function of the distortion energies calculated at the (a) PMP2/6-31G* and (b) G2 levels.

non-HF methods. The G2 value for this reaction is 14 kcal/mol, while the other methods predict values ranging from 6 kcal/mol (B3LYP/6-311+g**) to 22 kcal/mol (PMP2/6-31g*).

The highest activation barrier pathway by all methods is hydrogen exchange on carbon. The G2 method predicts this barrier to be 42 kcal/mol. All methods of calculation predict the next highest barrier to be hydrogen attack on carbon to form methane and hydroxyl with a G2 value of 32 kcal/mol.

Throughout all of these calculations, some trends are seen. The Hartree−Fock and Moller−Plesset methods always predict barriers that are about twice those of the G2 calculations. The density functional method always gives values about half as large as the G2 results. However, both MP4SDTQ(FC) basis sets and the QCISD(T) calculation give activation energies close to the G2 values. More importantly, if one would like to quickly identify reactivity trends, these two methods order the reactions the same way from highest to lowest activation energy as the G2 calculation without the computational cost of the G2 calculations.

The intrinsic activation barriers found by using the Bokris method for γ are shown in Table 1. Because the G2 method has been proven to be the best method for this reaction system, only values from it will be used for the remainder of this section. We see that both hydrogen abstraction reactions, reactions 4 and 5, have the lowest intrinsic activation barriers. Their values are 15 and 14 kcal/mol, respectively. However, attack on carbon in reactions 6 and 8 has a very high intrinsic activation barrier, around 40 kcal/mol. One would think that reactions 7 and 9 would have intrinsic barriers similar to one another, then, because both are hydrogen attack or oxygen reactions. However, hydrogen attack on oxygen for the exchange reaction has an intrinsic barrier of only 24 kcal/mol, as is seen for reaction 7. Reaction 9 has a value twice that at 38 kcal/mol. The origin of this barrier is unclear because reaction 9 is clearly favored to have a lower barrier through thermodynamic arguments.

Results: Distortion Energies

In the next part of the paper we will calculate the energy it takes to distort the bonds to reach the transition state. Recall that in previous work Mitchell et al.[10,11] found that there was a correlation between the barriers to reactions and the energy to distort bonds in calculations at the HF/4-31g level.

Mitchell's distortion energies were much higher than those we have found with larger basis sets.[13−15] Therefore, there is reason to recalculate the distortion energies.

The distortion energies were found using a procedure similar to that of Mitchell.[10,11] First we calculated the transition-state geometries for reactions 4−9 at the MP2/6-31g* level. Then the incoming hydrogen was removed and all geometric parameters were fixed to recalculate the energy at the PMP2 and G2 levels. We then define the distortion energy as

$$E_d = E(\text{distorted methanol}) - E(\text{ground-state methanol}) \quad (13)$$

where E(distorted methanol) is the energy of the methanol which has been distorted to the transition-state geometry and E(ground-state methanol) is the energy of an undistorted methanol. When we considered the reverse reaction, we calculated the energies for the reactants with the geometries they would need at the transition state. We subtracted their ground-state values from this to get E_d. Table 3 shows the results at the PMP2 level, while Table 4 shows the results at the G2 level. Table 5 shows the geometries for the products and reactants, while Table 6 has the transition-state geometries.

Notice that there is little correlation between the activation barriers and the energies to distort the molecules. This is in contrast to results of Mitchell et al.[10,11] In particular, Mitchell et al. found that the barriers calculated at the HF/4-31G level had a linear correlation with the distortion energies. Figure 2 shows plots of our results, and the correlation between the distortion energies is much poorer than that reported by Mitchell et al.

We also plot the overall activation energies versus distortion energies in Figure 3. Again, the correlation is much worse than seen in the HF/4-31G-calculations of Mitchell et al. Another difference is that Mitchell suggests that the barriers are always less than the distortion energies. Notice that our results for reactions 6−9 disagree with this. For example, in reaction 9, only the C−O bond is stretched significantly when we move to the transition state. It costs only 15 kcal/mol to distort the methanol to get to the transition-state geometry for reaction 9. By comparison, the activation barrier is 25 kcal/mol. All the reverse reactions also have barriers higher than their distortion energies.

However, we do have two cases where the activation barrier is less than the energy of distortion as Mitchell suggested. These are reactions 4 and 5. Once again, in reaction 4, only one bond was significantly stretched. Stretching the hydrogen−carbon bond leads to a distortion energy of 15 kcal/mol. Yet, reaction 4 has a barrier of 9 kcal/mol.

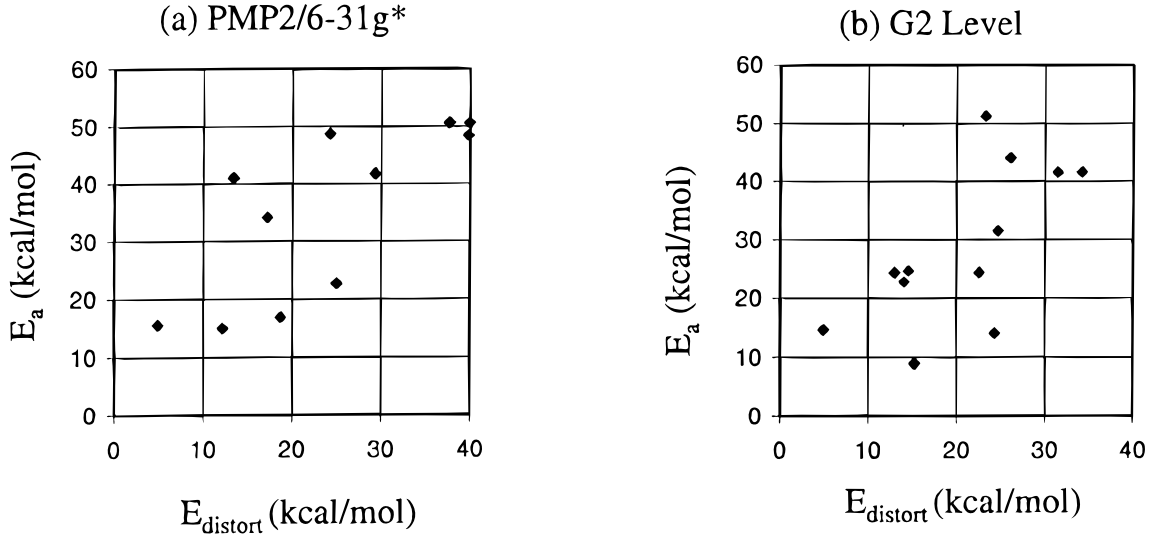

Figure 3. Plot of the calculated activation barriers for reaction as a function of the distortion energies calculated at the (a) PMP2/G-31G* and (b) G-2 levels.

TABLE 3: PMP2/6-31g* Results (kcal/mol)

	E_a	distortion	energy to bring reactants together	curve-crossing energy	energy of stretched bonds in products	Szabo energy
			Forward Reaction			
4	16.92	18.71	24.23	17.47	82.76	−65.29
5	22.69	25.00	27.71	24.79	87.03	−62.24
6	50.66	39.92	68.37	12.67	93.50	−80.83
7	41.00	13.39	44.83	11.21	89.74	−78.53
8	41.69	29.30	52.21	18.13	91.82	−73.69
9	34.17	17.21	40.54	16.91	89.39	−72.48
			Reverse Reaction			
4	15.55	4.91	24.44	9.91	87.54	−77.63
5	15.01	12.20	20.12	5.64	76.02	−70.38
6	50.66	37.61	68.37	12.67	93.50	−80.83
7	41.00	13.35	44.83	11.21	89.74	−78.53
8	48.44	39.77	66.88	17.54	83.00	−65.41
9	48.74	24.19	59.95	20.78	84.42	−63.64

TABLE 4: G2 Results (kcal/mol)

	E_a	distortion	energy to bring reactants together	curve-crossing energy	energy of stretched bonds in products	Szabo energy
			Forward Reaction			
4	8.99	15.27	19.18	14.38	98.01	−83.63
5	14.07	24.28	23.19	24.10	101.33	−77.23
6	41.55	34.17	56.23	10.02	98.06	−88.04
7	24.38	22.56	23.89	11.51	94.27	−82.76
8	31.54	24.67	42.93	15.43	97.58	−82.15
9	24.74	14.57	31.66	14.78	94.56	−80.18
			Reverse Reaction			
4	22.85	14.07	30.17	6.38	92.91	−86.53
5	14.71	4.96	17.10	3.07	81.60	−78.53
6	41.55	31.41	56.23	10.02	98.06	−88.04
7	24.38	12.98	23.89	11.51	94.27	−82.76
8	44.05	26.09	64.4	14.43	83.23	−68.8
9	51.26	23.26	56.91	18.44	84.47	−66.03

We cannot directly compare to Mitchell's numbers because we are using neutral radicals while Mitchell did his calculations with neucleophiles. It does not seem that the correlations reported by Mitchell et al., based on HF/4-31G calculations, carry over to the larger basis sets used here.

Results: Pauli Repulsions

In the previous section we showed that there was little correlation between the activation barriers and the distortion energies. Therefore, we needed to find another variable which correlates to our results. One possibility is that there would be a correlation to the energy to bring the reactants together. Recall that, even if bonds do not distort, it costs energy to move the reactants together because the electrons on one reactant repel the electrons on the other reactant. One can quantify this effect by defining E_p, the energy associated with the Pauli repulsions, by

$$E_p = E(\text{undistorted reactants at the transition state}) - E(\text{separated reactants}) \quad (14)$$

In eq 14 E(undistorted reactants at the transition state) is the energy of the reactants when the distance between the reactants is the same distance as in the transition state but all of the bonds in the reactants are at their equilibrium positions. The reactants were oriented in a way that minimized the electron−electron repulsions. E(separated reactants) is the energy of two separated reactants. Physically, E_p is the energy to push the reactants together without stretching or distorting bonds. Tables 3 and 4 show our calculated values of E_p. Tables 5 and 6 give reactant, product, and transition state geometries. Table 7 shows the geometries used to calculate E_p. Figure 4 shows a plot of activation barriers versus the Pauli repulsion energy. Unlike with distortion energies, there is a correlation between the energies to bring the reactants together and the barriers to reaction.

Results: Curve-Crossing Energies

A different idea in the literature is that barriers to reaction are associated with a curve-crossing on a potential energy surface. For example, Figure 5 shows a diagram of a curve-crossing model taken from Masel.[9] Similar diagrams are found in many other kinetics textbooks. During the reaction, a bond in the reactants stretches and breaks. Many investigators have suggested that the barrier for reaction is associated with the energy to stretch bonds to reach the transition-state.

Following Johnston,[1] we will define the energy of the curve-crossing, E_x, by

$$E_x = E(\text{reactant with a stretched bond}) - E(\text{ground-state reactant}) \quad (15)$$

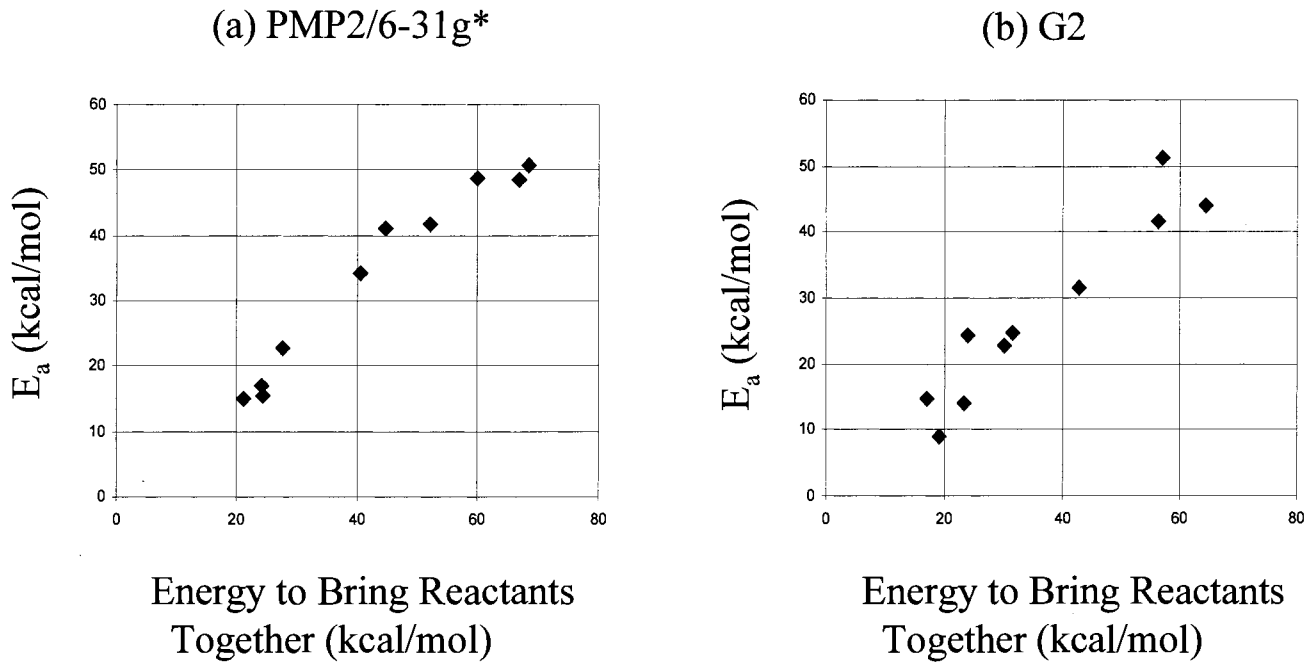

Figure 4. Plot of the activation barriers for reaction as a function of the energies to bring the reactants together calculated at the (a) PMP2/6-31G* level and (b) G2 level.

TABLE 5: Reactant and Product Geometries for H + CH_3OH → Products (Bond Lengths in Angstroms, Angles in Degrees

species	geom parameter	exptl	calcd
CH_3OH	C−H	1.0936	1.0943
	O−H	0.9451	0.97
	C−O	1.4246	1.423
	∠OH	108.53	109.285
	∠HCH	108.63	108.7963
CH_3	C−H	1.08	1.0783
	planar		
CH4	C−H	1.0870	1.0897
	Td		
H_2	H−H	0.7414	0.7376
H_2O	O−H	0.9575	0.969
	∠HOH	104.51	103.91
CH_3O	C−H	1.10	1.097
	C−O	1.37	1.3861
	∠HCO	NA	117.43
	∠HCH	109.0	104.83
CH_2OH	C−H	NA	1.0824
	C−O	NA	1.3731
	O−H	NA	0.9705
	∠HCO	NA	116.15
	∠HOC	NA	108.52
OH	O−H	0.971	0.9787

TABLE 6: Transition-State Geometries for H + CH_3OH → Products (Bond Lengths in Angstroms and Angles in Degrees)

products of H′ + CH_3OH →	geom parameter	calcd value
CH_3H' + OH	O−C	1.7136
	H−C	1.085
	H′−C	1.3528
	H−O	0.9759
	∠HCO	92.87
	∠HOC	102.56
CH_3 + OHH′	O−C	1.7008
	H−C	1.084
	H−O	0.982
	H′−O	1.2126
	∠HCO	105.05
	∠HOC	104.195
	∠H′OC	156.51
HH′ + CH_2OH	H′−H	0.9273
	$H_{abstracting}$−C	1.3734
	H−C	1.090
	O−C	1.3876
	O−H	0.9712
	∠HCO	111.83
	∠HOC	108.312
HH′ + CH_3O	H′−H	0.867
	H−O	1.249
	H−C	1.0953
	O−C	1.4106
	∠HCO	109.9
	∠HOC	106.79
H + $CH_2H'OH$	H′−C	1.2993
	∠$H_{leaving}$−C	1.3057
	H−C	1.0991
	O−C	1.441
	H−O	0.9733
	∠$H_{leaving}$CO	89.098
	∠HCO	120.18
	∠H′CO	96.33
	∠HOC	106.77
H + CH_3OH'	H′−O	1.1376
	H−O	1.138
	H−C	1.0875
	O−C	1.4827
	∠HCO	108.30
	∠HOC	109.01

where *E*(reactant with a stretched bond) is the energy from the BEBO plot (i.e., a plot of the bond energy versus bond length for the bond which breaks) at the transition-state bond length. Tables 3 and 4 show the energies of curve-crossing, while Figure 6 show a plot of the activation energies versus the curve-crossing energies.

Notice that there is little correlation between the curve-crossing energies and the barriers to reaction. Evidently the curve-crossing model, like the distortion energy model, does not apply to our reactants.

Results: Szabo Energies

Activation barriers might also be correlated with a modification of the curve-crossing model introduced by Szabo.[3] Szabo suggested that the curve-crossing model gives incorrect results

TABLE 7: Geometries Used To Calculate the Energy To Bring Reactants Together (Bond Lengths in Angstroms and Angles in Degrees)

forward reactions, products of $H' + CH_3OH \rightarrow$	geom parameter	calcd value	backward reactions, reactants $\rightarrow H' + CH_3OH$	geom parameter	calcd value
$CH_3H' + OH$	O−C	1.4230	$CH_3H' + OH$	H−C	1.0897
	H−C	1.090		O−C	1.7136
	H′−C	1.3528		H−O	0.9791
	H−O	0.9700		∠HCH′	109.47
	∠HCO	107.40		∠OCH′	164.88
	∠HOC	109.00		∠HOC	110.40
$CH_3 + OHH'$	O−C	1.4230	$CH_3 + OHH'$	H−C	1.0783
	H−C	1.090		H−O	0.969
	H−O	0.9700		O−C	1.7007
	H′−O	1.2126		∠HCO	90.0
	∠HCO	109.00		∠HOC	120.0
	∠HOC	107.37		∠HOH′	103.91
	∠H′OC	156.52		∠HCH	120.0
$HH' + CH_2OH$	H′−H	0.9273	$HH' + CH_2OH$	H′−H	0.7376
	H−C	1.090		H−C	1.083
	O−C	1.423		O−C	1.373
	O−H	0.9700		O−H	0.9705
	∠HCO	109.00		$H_{entering}$−C	1.3734
	∠HOC	107.37		∠HOC	108.52
				∠HCO	116.17
				∠H′$H_{entering}$	178.19
$HH' + CH_3O$	H′−H	0.8670	$HH' + CH_3O$	H−C	1.097
	H−O	0.9700		O−C	1.3873
	H−C	1.0900		O−H	1.3783
	O−C	1.4230		H′H	0.7376
	∠HCO	109.00		∠HCO	108.4
	∠HOC	107.37		∠HOC	106.79
	∠H′HO	180.0		O−C	1.3873
$H + CH_2H'OH$	H′−C	1.2993	$H + CH_2H'OH$	H′−C	1.2993
	H−C	1.0900		H−C	1.0900
	O−C	1.4230		O−C	1.4230
	H−O	0.9700		H−O	0.9700
	∠HCO	109.00		∠HCO	109.00
	∠H′CO	96.33		∠H′CO	96.33
	∠HOC	107.37		∠HOC	107.37
$H + CH_3OH'$	H′−O	1.1376	$H + CH_3OH'$	H′−O	1.1376
	H−O	0.9700		H−O	0.9700
	H−C	1.0900		H−C	1.0900
	O−C	1.4230		O−C	1.4230
	∠HCO	109.00		∠HCO	109.00
	∠HOC	107.37		∠HOC	107.37

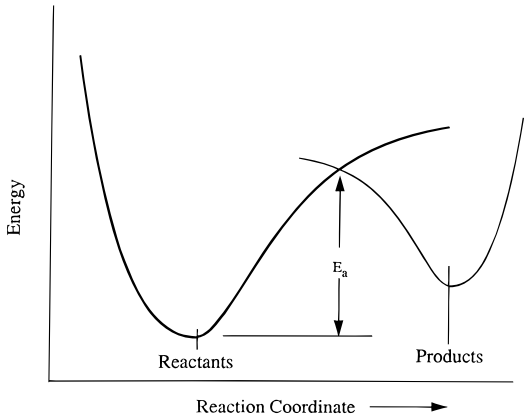

Figure 5. Activation energy according to the curve-crossing model.

because, at every point on the reaction coordinate, a new bond is forming as well as an old one breaking. Following Szabo, we will define a Szabo energy, E_s, by

$$E_s = E_x + E(\text{product with a stretched bond}) \qquad (16)$$

Again, Tables 3 and 4 give numerical values of the Szabo energies while Figure 7 plots the activation barriers versus the Szabo energies. Notice that all of the Szabo energies are negative, which means that Szabo's analysis would suggest that all of the reactions are unactivated. Further, there is little correlation between E_s and the barriers to reaction. Much like the curve-crossing model, activation barriers do not correlate with Szabo's modification.

Results: Effects of Complexes

So the only phenomena that correlates well with activation energy in this work is the energy to bring the reactants together. The distortion energies, curve-crossing energies, and Szabo energies show no correlation with activation energy.

The presence of complexes within the product and reactant pathways was also examined. All reactant complexes were within 1 kcal/mol the infinitely separated reactant energies. Product complexes, though, varied by as much as 27 kcal/mol from the separated energies.

Plots were made using the complexes as the basis for the activation energy, heats of reaction, and intrinsic barriers. Figure 8 shows E_A versus $E_{distort}$ including the complexes. The other energies were also modified appropriately. None of the correlations improved. The distortion energy, curve-crossing energy, and Szabo energy still did not correlate with activation barriers. And, in fact, the correlation between the energy to bring the reactants together and activation energy was slightly worse.

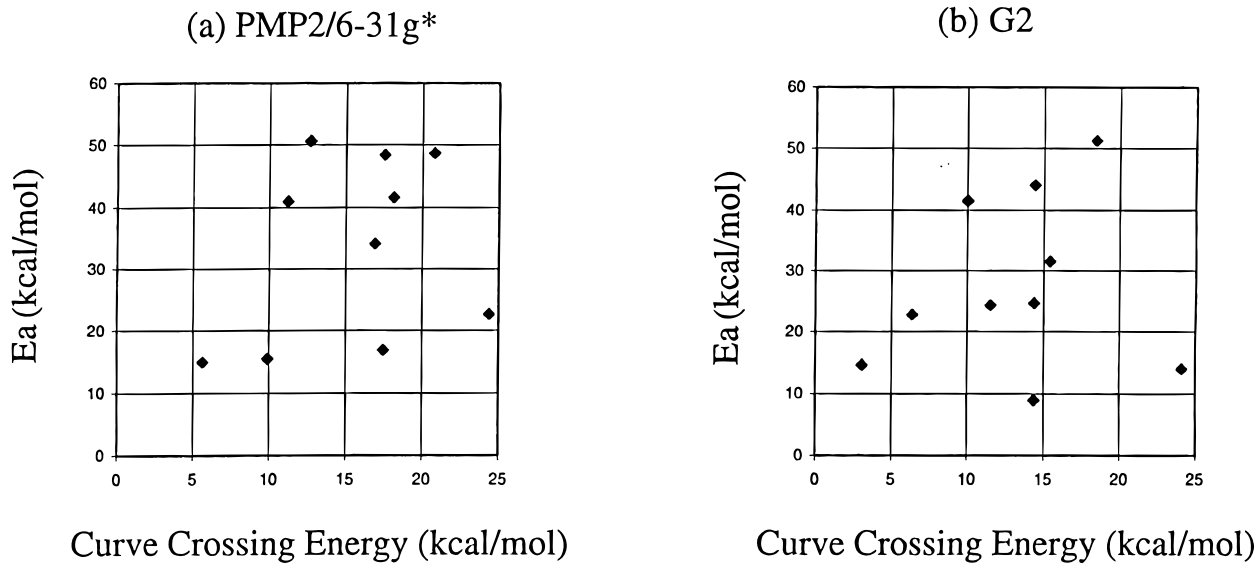

Figure 6. Plot of the activation barriers to reaction versus the curve-crossing energy calculated at the (a) PMP2/631G* and (b) G2 levels.

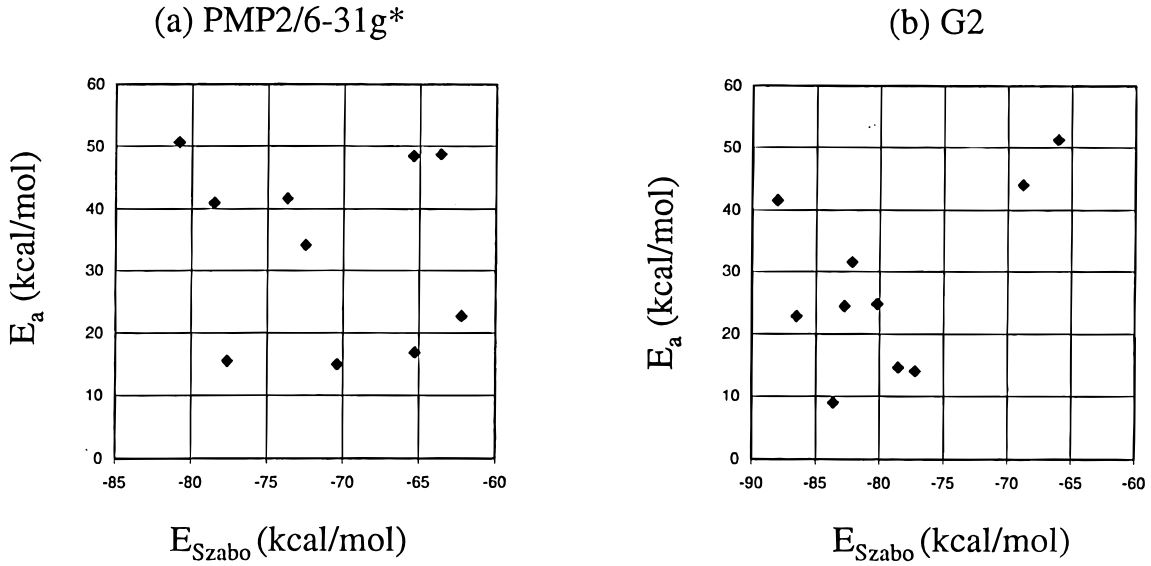

Figure 7. Plot of the activation barrier to reaction versus the Szabo energies calculated at the (a) MP2/6-31G* and (b) G-2 levels.

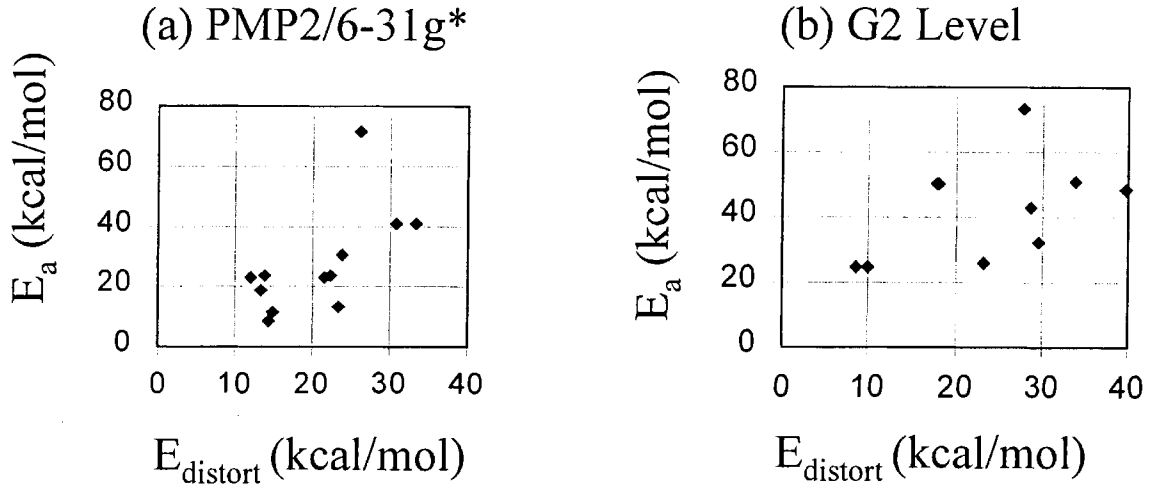

Figure 8. Plot of the calculated activation barriers for reaction as a function of the distortion energies calculated at the (a) PMP1/6-31g* and (b) G2 levels with complexes included.

Discussion

The results here were unexpected based on the previous work. In the previous literature, people have often discussed barriers to reaction in terms of the energies to bring the reactants to the curve-crossing. However, Figure 6 shows that the curve-crossing energy has little correlation to the barriers to reaction.

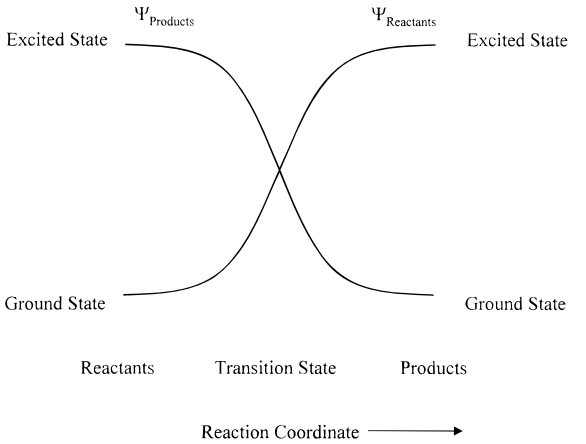

Figure 9. Correlation diagram used to derive the curve-crossing model.

Similarly, people have discussed barriers in terms of the energies to 13 distort bonds. In particular, Mitchell et al.[10,11] found a correlation between barriers to reaction and the distortion energies using HF/4-31G calculations. However, in contrast to Mitchell's results, our results in Figures 2 and 3 show little correlation between the barriers to reaction and the distortion energies. In our case, we find that the nature of the wavefunctions changes as we move toward the transition-state. In particular diffuse functions have much larger contributions to the transition-state than to reactants and products. Mitchell et al. did not have diffuse functions in their calculations, which is one of the key reasons his results were so much different from ours.

The one variable with which our data did correlate was the energy to bring the reactants together. Figure 4 shows this correlation. Notice how well the activation energy correlates with the energy to bring the reactants together. As a result, we suggest that the main barriers to reaction are associated with the energies to bring the reactants together, and not the energies to distort bonds.

We can speculate why the curve-crossing model failed. The standard derivation of the curve-crossing model starts with a correlation diagram like that in Figure 9. During the reaction, some of the excited states of the reactants are transformed into states of the products and vice versa. According to the curve-crossing model, the reaction can be viewed as a curve-crossing between reactant and product configurations.

Note, however, that there is an inherent assumption in the curve-crossing model that there is a two level system; i.e., only states which are present in the reactants or products contribute to the transition-state. Such an assumption works in a minimum basis set calculation. However, this assumption does not work in our calculations. We find that diffuse functions make major contributions to the transition state even though the diffuse functions do not make a significant contribution to the reactants and products.

Physically, orbitals are getting distorted when the reactants come together. For example, Figure 10 shows a diagram of the changes in the 6A′ orbital during reaction 8. To put the figure in perspective, note that there is often a uniqueness problem in drawing orbital diagrams. However, it happens that reaction 8 occurs in a very symmetrical environment. The symmetry eliminates some of the difficulties with uniqueness. Uniqueness was a problem for the other reactions, so we only show orbital diagrams for reaction 8.

Figure 11 shows that the 1S orbital on the hydrogen starts out spherical, while the 6A′ orbital on the methanol starts out

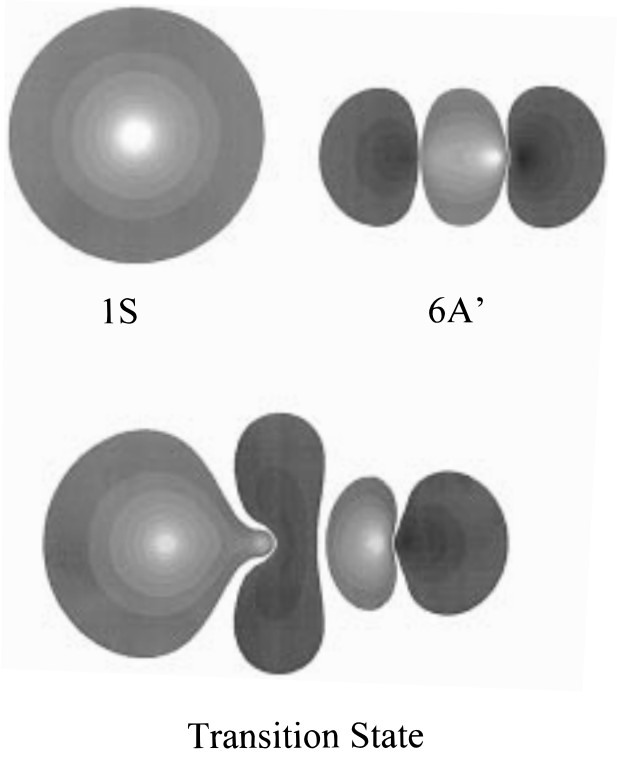

Figure 10. Changes in the 6A′ orbital during reaction 8.

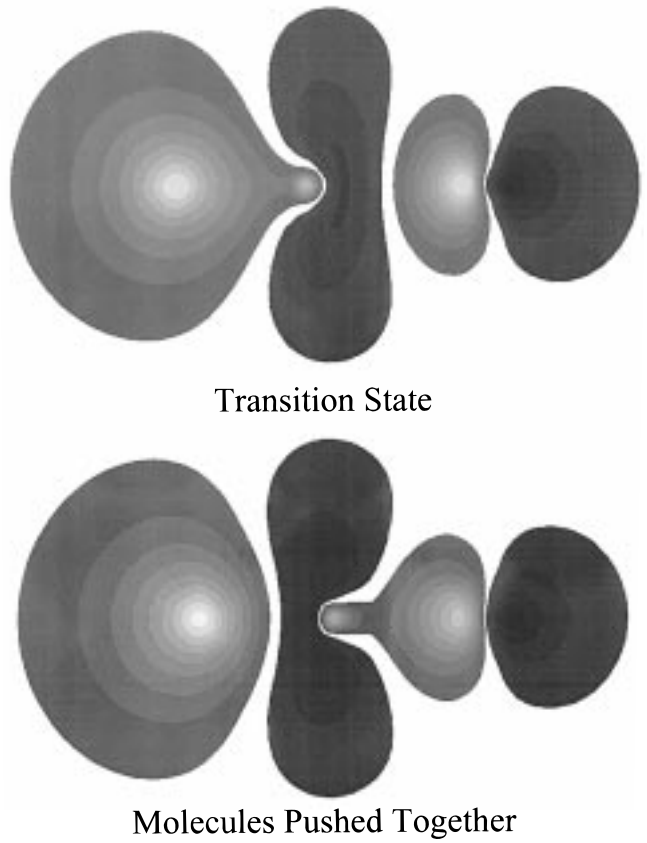

Figure 11. Changes in the 6A′ orbital when the reactants come together but no bonds stretch.

with a kidney-shaped lobe pointing toward the hydrogen. When the reactants come together, the 1S orbital flattens and squishes out the sides, while the 6A′ orbital flattens as the C−H bonds distort.

Notice that there are significant orbital distortions during the

reaction. The orbitals in the transition state do not look like orbitals in the reactants or products. Instead there are significant contributions from basis functions that are not present in the reactants or products. As a result, the curve-crossing model fails.

In contrast, when we move the reactants together without distorting bonds, we get the orbitals shown in Figure 11. The orbitals in Figure 11 look very similar to those in Figure 10. Since the orbitals are similar, the energy to move the reactants together is a good representation of the changes which occur when the reaction happens. Consequently, barriers to reaction correlate well with the energy to bring the reactants together. This result suggests that most of the barriers to reaction are associated with the energies to bring the reactants together and not the energies to stretch or distort bonds.

Next, we want to focus on the idea that Pauli repulsions are the underlying cause of bond stretching and distortion. As the reactants approach one another, the electron clouds encounter each other and are repulsed. The breaking bond begins to stretch as the forming bond becomes shorter. In addition, the other atoms are pushed out of the way to make room for the incoming species. The end effects of the electron−electron repulsions are bond stretching, bond distortion, and the molecular orbital changes that accompany them. All of these effects happen in a concerted manner throughout the reaction. However, addressing each phenomenon separately allows us to see which one contributes most to, and correlates with, the activation barrier. So, we see that the energy to bring the reactants together without distortion correlates best with activation energy.

Next, we want to point out that the energy to bring the reactants together without distortion is larger than the barriers to reaction. Physically, according to the variational principle, when we bring the reactants together without allowing bonds to stretch or distort, the energy is higher than if we allow bond distortions to occur. Thus, bond distortions lower the barriers to reaction. This leads us to a surprising conclusion. *Bond stretching and bond distortion always lower the barriers to reaction.*

Physically, the reactants must be brought together before reaction occurs. The results here show that there is a significant barrier to bringing the reactants together and that the barrier to bringing the reactants together controls the barrier to reaction. From the variational principle, bond distortion and bond stretching always lower the barriers to reaction. Therefore, we believe that, at least in the cases considered here, it is incorrect to think of barriers as being associated with bond stretching and distortion. Rather, the main barrier is associated with the Pauli repulsions in moving the reactants together. The bond distortions always relieve the stresses caused by bringing the reactants together. Therefore, bond distortion always lowers, rather than raises, the barriers to reactions.

One of the questions one has to ask is whether the results here are general or specific to our reaction system and our way of calculating energies. We do not believe that the results are artifacts associated with our computational procedures. We have done calculations with a variety of different calculational procedures and basis sets as indicated in the supplemental material. Our key findings are largely independent of our computational methods, provided we include diffuse functions in our basis set. Therefore, they are unlikely to be associated with a computational artifact.

We are not sure whether our results are special to reactions 4 through 9. However, they are all radical reactions of neutral species. If we had used charged species instead, the energies to move the reactants together would be different than with the uncharged species. That would certainly affect our findings. Charge transfer in the transition state could also change our findings because its effect in all of the reactions considered here is small. Still, we would expect the results here to apply to a wide variety of reactions.

Conclusions

In this paper we used ab initio methods to calculate the barriers for a series of reactions between methanol and hydrogen. We find that the activation energy shows little correlation with either the energy to distort the reactants to the transition-state geometry or the energy to stretch bonds to the curve-crossing in the potential energy surface. There is a good correlation between the energy to bring the reactants together and the activation barriers to reaction.

Physically, the orbitals in the reactants are distorted when the reactants come together. The distorted wave functions have contributions from states which do not contribute significantly to either the reactants or products. In our reactions, the orbital distortions lead to the barriers to reaction. In contrast, bond stretching and bond distortion lower these barriers. We do not know whether the results are general or special to our reactions. However, our results were certainly unexpected based on what has been said about similar reactions in the past.

Acknowledgment. This work was funded by NSF Grant Number CTS 96 10115.

Supporting Information Available: A table of energies of all transition states, products, and reactants at all levels of calculation (1 page). See any current masthead page for ordering and Internet access information.

References and Notes

(1) Johnston, H. Gas Phase Reaction Rate Theory; Ronald: New York, 1966.
(2) Evans, M. G.; Polanyi, M. *Trans. Faraday Soc.* **1938**, *34*, 11.
(3) Szabo, Z. G.; Berces, T. Z. *Phys. Chem.* **1968**, *57*, 113.
(4) Glasstone, S. The Theory of Rate Processes; McGraw-Hill: New York, 1941.
(5) Pellerite, M. J.; Brauman, J. I. *J. Am. Chem. Soc.* **1983**, *105*, 2672.
(6) Laidler, K. J. *Chemical Kinetics*; McGraw-Hill: New York, 1965.
(7) Steinfeld, J.; Francisco, J.; Hase, W. *Chemical Kinetics and Dynamics*; Prentice-Hall: New York, 1989.
(8) Moore, J.; Pearson, R. *Kinetics and Mechanism*; Wiley and Sons: New York, 1981.
(9) Masel, R. I. *Principles of Adsorption and Reaction on Solid Surfaces*; J. W. Wiley and Sons: New York, 1996.
(10) Mitchell, D. J.; Schlegel, H. B.; Shaik, S. S.; Wolfe, S. *Can. J. Chem.* **1985**, *63*, 1642.
(11) Wolfe, S.; Mitchell, D. J.; Schlegel, H. B. *J. Am. Chem. Soc.* **1981**, *103*, 7692.
(12) Goddard, W. A.; Ladner, R. C. *J. Am. Chem. Soc.* **1971**, *93*, 6750.
(13) Lee, W. T.; Masel, R. I. *J. Catal.* **1997**, *165*, 80.
(14) Lee, W. T.; Masel, R. I. *J. Phys. Chem.* **1996**, *100*, 10945.
(15) Lee, W. T.; Masel, R. I. *J. Phys. Chem.* **1995**, *99*, 9363.
(16) Dzotnidze, *Arm. Kim. Zh.* **1968**, *21*, 370.
(17) Westley, F. *Tables of Recommended Rate Constants for Reactions Occurring in Combustion*; NBS: Washington, DC, 1980.
(18) Yagasaki, E.; Masel, R. I. *J. Am. Chem. Soc.* **1990**, *112*, 8746.
(19) Franaszczuk, K.; Herrero, E.; Zelenay, P.; Wieckowski, A.; Wang, J.; Masel, R. I. *J. Phys. Chem.* **1992**, *96*, 8509.
(20) Wang, J.; Masel, R. I. *J. Am. Chem. Soc.* **1991**, *113*, 5850.
(21) Shah, R.; Payne, M. C.; Lee, M. H.; Gale, J. D. *Science* **1996**, *271*, 1395.
(22) Frish, M. J.; Trucks, G. W.; Schlegel, H. B.; Gill, P. M. W.;

Johnson, B. G.; Wong, M. W.; Foresman, J. B.; Robb, M. A.; Head-Gordon, M.; Replogle, E. S.; Comperts, R.; Andres, J. L.; Raghavachari, K.; Binkley, J. S.; Gonzalez, C.; Martin, R. L.; Fox, D. J.; Defrees, D. J.; Baker, J.; Stewart, J. J. P.; Pople, J. A. *Gaussian 92/DFT, Revision G.2*; Gaussian, Inc.: Pittsburgh, PA, 1993.

(23) Frish, M. J.; Trucks, G. W.; Schlegel, H. B.; Gill, P. M. W.; Johnson, B. G.; Robb, M. A.; Cheeseman, J. R.; Keith, T.; Peterson, G. A.; Montgomery, J. A.; Raghavachari, K.; Al-Laham, M. A.; Zakrzewski, V. G.; Ortiz, J. V.; Foresman, J. B.; Peng, C. Y.; Ayala, P. Y.; Chen, W.; Wong, M. W.; Andres, J. L.; Replogle, E. S.; Gomperts, R.; Martin, R. L.; Fox, D. J.; Binkley, J. S.; Defrees, D. J.; Baker, J.; Stewart, J. J. P.; Head-Gordon, M.; Gonzales, C.; Pople, J. A. Gaussian 94, Revision B.3; Gaussian, Inc.: Pittsburgh, PA, 1995.

(24) Curtiss, L. A.; Raghavachav, K.; Trucks, G. W.; Pople, J. A. *J. Chem. Phys.* **1991**, *94*, 7221.

(25) Evans, M. G.; Polanyi, M. *J. Chem. Soc., Faraday Trans.* **1936**, *32*, 133.

(26) Bokris, J. O. *Modern Electrochemistry*; Plenum: New York, 1970, Vol. 2, p 1110.

(27) Nguyen, M. T.; Creve, S.; Vanquichenborne, L. G. *J. Phys. Chem.* **1996**, *100*, 18422.

(28) Torrent, M.; Duran, M. *J. Mol. Struct.* **1996**, *362*, 163.

(29) CRC Handbook of Chemistry and Physics, 73rd ed.; Lide, D. R., Ed.; CRC Press: Boca Raton, FL, 1992−1993.

(30) Liu, Xi, Damo, C. P.; Lin, T.-Y. D.; Foster, S. C.; Misra, P.; Yu, L.; Miller, T. A. *J. Phys. Chem.* **1989**, *93*, 2266.